Examination of the $^2A_2'$ and $^2E''$ states of NO_3 by ultraviolet photoelectron spectroscopy of NO_3^-

A. Weaver,[a] D. W. Arnold,[b] S. E. Bradforth,[c] and D. M. Neumark[d]
Department of Chemistry, University of California, Berkeley, California 94720

(Received 13 July 1990; accepted 22 October 1990)

The photoelectron spectrum of the NO_3^- anion has been obtained at 266 and at 213 nm. The 266 nm spectrum probes the $^2A_2'$ ground state of NO_3. The 213 nm spectrum represents the first observation of the $^2E''$ lowest-lying excited state of NO_3. The $^2A_2'$ band shows vibrational progressions in the ν_1 symmetric stretch and the ν_4 degenerate in-plane bend of NO_3. Our analysis of this band indicates that the NO_3 ground state has a D_{3h} equilibrium geometry and is vibronically coupled to the $^2E'$ second excited state via the ν_4 mode. We also obtain the electron affinity of NO_3, 3.937 ± 0.014 eV, and the heat of formation of NO_3 at 298 K, 0.777 ± 0.027 eV (17.9 ± 0.6 kcal/mol). The $^2E''$ state of NO_3 lies 0.868 ± 0.014 eV above the ground state. The $^2E''$ band shows complex and extensive vibrational structure. Several possible assignments of this structure are discussed.

I. INTRODUCTION

Nitrogen trioxide, NO_3, is one of the most important free radicals in atmospheric chemical reactions. As one of the NO_x species, it is implicated in reaction cycles involving ozone and in hydrocarbon and halocarbon oxidation.[1] Although NO_3 is rapidly photolyzed during the day, it is essential to the cycle of reactions which form HNO_3 at night and is thus an important contributor to acid precipitation.[2] The significance of NO_3 in atmospheric chemistry has prompted numerous spectroscopic and kinetic experiments and theoretical studies, but questions remain concerning its ground state structure, excited electronic states, and photochemistry. In this paper, we use photoelectron spectroscopy of NO_3^- to address two of these issues: the geometry of the ground electronic state and characterization of the first excited electronic state of NO_3.

Walsh[3] predicted that NO_3 would be planar with a threefold symmetry axis (D_{3h} point group) in the ground electronic state and first two excited states ($^2A_2'$, $^2E''$, and $^2E'$, respectively). The proposed threefold symmetry of the ground state has been disputed. Rotationally resolved infrared spectra[4–6] of the ground state support Walsh's prediction of a $^2A_2'$ ground state with D_{3h} symmetry, but vibrationally resolved dispersed fluorescence spectra have been interpreted as evidence of either D_{3h}[7] or Y-shaped planar[8] (C_{2v}) structure by different researchers. *Ab initio* predictions of the ground state equilibrium geometry are divided between D_{3h}[9–13] and C_{2v}[11,14–18] symmetry. Discrepancies between these predictions are partly due to the inherent difficulty of treating NO_3 properly, since it is an open-shell molecule with partial double bonds and low-lying excited electronic states.

Considerably less is known about the excited electronic states of NO_3. The only electronic transition that has been observed is the $^2E' \leftarrow {}^2A_2'$ band, with its origin at 662 nm. This band has been studied using absorption[19–21] and fluorescence excitation[7,8,22] spectroscopy, but the diffuse vibrational structure evident in these spectra has not been fully analyzed. Johnston and co-workers[23] see no rotational structure in this band even at 0.007 cm^{-1} resolution. The $^2E''$ state is predicted to lie between the ground state and the $^2E'$ state[3,11,16,24–26] but has not been observed because the $^2E'' \leftarrow {}^2A_2'$ transition is electric-dipole forbidden. The exact energy of the $^2E''$ state is important because some features of the ground-state spectrum have been attributed to perturbations by a low-lying electronic state, but *ab initio* predictions of its energy vary from 0.04 eV (300 cm^{-1})[16] to 1.61 eV (13 000 cm^{-1})[11] above the ground state.

We present here ultraviolet photoelectron spectra of the nitrate anion, NO_3^-, which provide new information about the ground state of NO_3 and represent the first direct observation of the $^2E''$ state. We observe the "dark" $^2E''$ state because negative ion photodetachment experiments can generally study all neutral electronic states formed by removing a single valence electron from the ion. The anion is expected to have a D_{3h} equilibrium geometry,[10,12,27,28] with the molecular orbital configuration $\ldots(e'')^4(e')^4(a_2')^2$ in the $^1A_1'$ ground state.[3] The $^2A_2'$, $^2E''$, and $^2E'$ electronic states of the NO_3 radical, which have the configurations $\ldots(e')^4(e'')^4(a_2')$, $\ldots(e')^4(e'')^3(a_2')^2$, and $\ldots(e')^3(e'')^4(a_2')^2$, respectively, are all accessible via one-electron photodetachment transitions from the ground state of NO_3^-. Our spectra show distinct bands corresponding to the $^2A_2'$ and $^2E''$ states of NO_3, which yield the electron affinity of NO_3 and the energy of the previously unobserved $^2E''$ excited state. With the laser currently in use, the $^2E'$ state is beyond the range of our photoelectron spectrometer.

The photoelectron spectra show vibrational progressions within each electronic band which provide new information about the frequencies and molecular geometry in the $^2A_2'$ and $^2E''$ states. In particular, these progressions indicate that vibronic coupling is important in both electronic states. Normally, the relative intensities of vibrational tran-

[a] NSERC (Canada) Postgraduate Scholar.
[b] NSF Predoctoral Fellow.
[c] University Fellow, University of California.
[d] NSF Presidential Young Investigator and Alfred P. Sloan Fellow.

 0021-9606/91/031740-12$03.00

sitions within a single electronic band in a photoelectron spectrum depend only on the Franck–Condon overlap of neutral and anion wave functions for the relevant vibrational states.[29] The longest progressions generally occur in totally symmetric vibrational modes of the neutral. For NO_3 in D_{3h} symmetry, the symmetric stretch (ν_1) is the only such mode. Progressions in non-totally symmetric modes may occur, but normally the only allowed transitions are those involving even changes in vibrational quantum number (even Δv transitions) between the anion and neutral. If the anion or neutral electronic state is degenerate, however, vibronic coupling due to the Jahn–Teller effect[30,31] can complicate the photoelectron spectrum. For example, odd Δv transitions can occur in non-totally symmetric vibrational modes. Such effects have been observed in photoelectron spectra of CH_3O^-,[32,33] and $C_5H_5^-$,[34] and in photoelectron spectra of neutral molecules such as BF_3[35–37] and CH_4.[38]

The $^2E''$ and $^2E'$ states of NO_3 are both degenerate, and the ν_3 antisymmetric stretch and ν_4 in-plane deformation can be Jahn–Teller active in each state. Our photoelectron spectra do provide evidence of vibronic coupling in the $^2E''$ state. However, we also observe what appear to be $\Delta v_4 = 1$ transitions in the ground state ν_4 progression. This is somewhat surprising, since the $^2A_2'$ state is nondegenerate and should not be affected by first-order Jahn–Teller coupling. This observation is discussed at length below, and is ultimately attributed to pseudo-Jahn–Teller coupling between the $^2A_2'$ and $^2E'$ states. This mechanism has previously been invoked by Haller *et al.*[36,37] to explain similar phenomena in the photoelectron spectrum of the isoelectronic molecule BF_3.

II. EXPERIMENT

The time-of-flight photoelectron spectrometer used in these experiments is shown in Fig. 1 and briefly described here. (See Ref. 39 for a more detailed description.) Negative ions are generated by crossing the free jet expansion from a pulsed molecular beam valve (1) with a 1 keV electron beam (2). For the NO_3^- spectra presented here, we used a gas mixture made by bubbling 5% NF_3 in argon through HNO_3 (red fuming, 90%). We also made NO_3^- from a 1% N_2O_4/He mixture, and obtained very similar spectra. The principles of operation of the ion source have been discussed at length by Johnson and Lineberger.[40] Electron impact ionization of the argon carrier gas generates low energy secondary electrons, which efficiently produce F^- from NF_3 by dissociative attachment. The subsequent exothermic proton transfer reaction of F^- with HNO_3 forms NO_3^-. The ions are formed in the continuum flow region of a free jet expansion, so they are expected to cool internally as the expansion progresses. We have measured vibrational temperatures of 100–150 K for CH_2CN^- produced in this source, and a rotational temperature of about 75 K for SH^- in a similar source.[41]

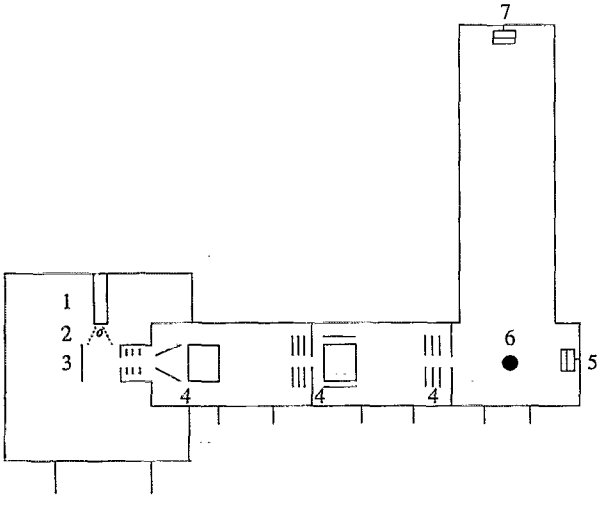

FIG. 1. Schematic of time-of-flight photoelectron spectrometer.

A 200–400 V negative pulse applied at (3) extracts the negative ions into a time-of-flight mass spectrometer.[42] The ions are accelerated to 1 keV, and ion deflectors and lenses (4) are adjusted to ensure optimal ion levels at the detector (5). Ions separate into bunches according to mass as they travel along the 150 cm flight tube, and the ion of interest is selectively photodetached (6) by varying the delay between ion extraction and the firing of the photodetachment laser. The signal level of negative ions, plus fast neutrals resulting from photodetachment, is monitored with a 25 mm dual microchannel plate detector. The neutral signal alone can be measured at this detector by applying -1400 V to a grid in front of the detector.

Photoelectrons are detected at the end of a 1 m flight tube by a 40 mm dual microchannel plate detector (7) and are energy analyzed by time of flight. We detect 0.01% of the ejected photoelectrons; this fraction is determined by the solid angle subtended by the electron detector. The instrumental resolution is 0.008 eV (64 cm^{-1}) at 0.65 eV electron kinetic energy, and degrades as $E^{3/2}$ at higher energy. The resolution in the spectra presented here is somewhat worse due to space charge effects (see below), and is 0.018–0.025 eV for electron kinetic energies near 1 eV. Rotational peaks are not resolved in the NO_3^- photoelectron spectra.

Spectra of NO_3^- were taken using the fourth (266 nm, 4.66 eV) and fifth (213 nm, 5.83 eV) harmonics of a Nd:YAG laser. The laser light is plane polarized, and the polarization at each wavelength can be rotated with a half-wave plate. Each spectrum shown here was averaged for about 500 000 laser shots, at 20 Hz repetition rate. The spectra were smoothed by convolution with Gaussian peaks of 6 meV FWHM. A background noise spectrum was subtracted from the 213 nm spectrum, to remove the photoelectron signal generated by stray laser photons which strike the metal surfaces of the chamber.

III. RESULTS

Photoelectron spectra of NO_3^- at 266 and 213 nm are shown in Figs. 2 and 3, respectively. The spectra are plotted as intensity (number of photoelectrons) vs electron kinetic energy (eKE). The electron energy is given by

$$eKE = h\nu - EA - T_0 - E_v^{(0)} + E_v^{(-)}. \quad (1)$$

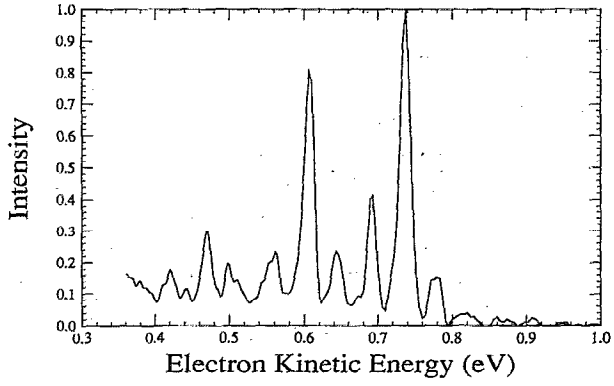

FIG. 2. Photoelectron spectrum of NO_3^- at 266 nm, showing the progression in the $^2A_2'$ state of NO_3. Laser polarization angle $\theta = 90°$.

where $h\nu$ is the photodetachment laser energy, EA the electron affinity of NO_3, T_0 the term value for the particular NO_3 electronic state, and $E_v^{(0)}$ and $E_v^{(-)}$ the vibrational energy of the neutral and anion, respectively. (We neglect the rotational contribution to the internal energy.) Peaks at highest electron kinetic energy correspond to transitions to the lowest electronic and vibrational energy levels of NO_3.

The 266 nm spectrum shows a single band with well-resolved vibrational structure. The peak positions are listed in Table I. The 213 nm spectrum shows this band at higher energy (hence poorly resolved), plus a band at lower electron energy with extensive vibrational structure. Peak positions of this second band are listed in Table II. Each band represents a series of transitions to vibrational levels within one electronic state of NO_3. The band in the 266 nm spectrum is assigned to the $^2A_2'$ ground state of NO_3, and the band at lower electron energy in the 213 nm spectrum is assigned to the $^2E''$ first excited electronic state. If we assign the peaks at 0.738 eV in the 266 nm spectrum and 1.035 eV in the 213 nm spectrum to the origins of the $^2A_2'$ and $^2E''$ progressions, respectively, we calculate T_0 for the $^2E''$ state to be 0.868 ± 0.014 eV (7000 ± 110 cm^{-1}).

Our results indicate a strikingly low partial photodetachment cross section into the $^2A_2'$ state of NO_3 at both 266 and 213 nm. The integrated intensity of the $^2A_2'$ state progression in the 213 nm spectrum is ten times less than that of the $^2E''$ state progression. This effect is independent of laser polarization angle (see below). In addition, our photoelectron signal levels were exceptionally low at 266 nm, where only the $^2A_2'$ state is accessible, and we photodetached only 2% of the ions (estimated by comparing the fast neutral signal to the ion signal) with a laser fluence of 120 mJ/cm^2. At 213 nm, where detachment to the $^2E''$ state dominates, we photodetached nearly 50% of the ions at a lower laser fluence of 60 mJ/cm^2 and the same ion level. This higher detachment rate is more typical of our experience with other ions.

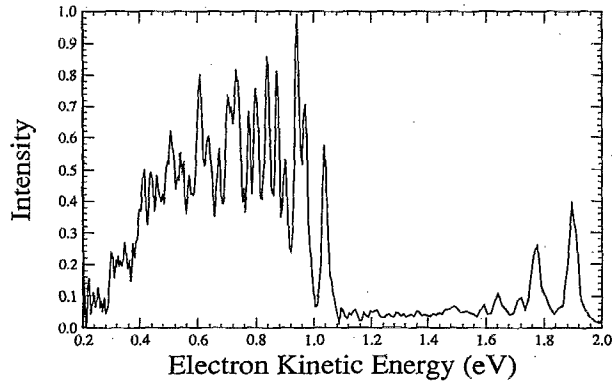

FIG. 3. Photoelectron spectrum of NO_3^- at 213 nm, showing progressions in the $^2A_2'$ and $^2E''$ states of NO_3. Laser polarization angle $\theta = 0°$.

TABLE I. Peak positions, 266 nm spectrum. Average uncertainty is 0.010 eV (80 cm^{-1}). Peak positions are not corrected for space charge (see text).

Position	
eV	cm^{-1}
0.820	− 661
0.780	− 339
0.738	0
0.693	363
0.644	758
0.607	1057
0.562	1420
0.511	1831
0.498	1936
0.470	2162
0.442	2387
0.421	2557

The low cross section for the $^2A_2'$ state required high ion densities to ensure adequate electron signal at 266 nm, and we obtained the 213 nm spectra at the same ion density. The peaks in our spectra were slightly broadened and shifted to higher energy by the resulting space charge effects, which arise from Coulomb repulsion between photoelectrons and the negative ion cloud. To estimate the magnitude of this shift, we took spectra of Br^- at 266 nm at comparable ion levels, since its mass and electron affinity (3.365 eV[43]) are relatively close to those of NO_3^-. We estimate that the peak at 0.738 eV in the NO_3^- 266 nm spectrum shifted by + 0.010 eV from its true position. This shift is approximately constant across the photoelectron spectrum, so the electron affinity is the only parameter affected. We obtain a value of 3.937 ± 0.014 eV for the electron affinity of NO_3, in good agreement with the most recent previous estimate of 3.91 ± 0.24 eV.[44]

The heat of formation of NO_3 at 298 K can be estimated from our electron affinity and the measured heat of formation of NO_3^-:

$$\Delta_f H°(NO_3)_{298\ K} = \Delta_f H°(NO_3^-)_{298\ K} + EA(NO_3) + \tfrac{5}{2}RT + \int_0^{298} [C_p(NO_3) - C_p(NO_3^-)] \qquad (2)$$

where the $5/2\,RT$ (= 1.481 kcal/mol) term corrects for the

TABLE II. Peak positions and intensities of $^2E''$ band, 213 nm spectrum. Average uncertainty at peak positions is 0.010 eV.

Position (experimental)					
eV	cm^{-1}	v_1[a]	v_4	Position[a] (calculated)	Intensity[b]
1.035	0	0	0	1.035	0.57
0.970	524	0	1	0.968	0.70
0.942	750	1	0	0.935	1.00
0.900	1089	0	2	0.901	0.53
0.871	1323	1	1	0.868	0.83
		2	0	0.836	
0.838	1589	0	3	0.834	0.87
0.798	1912	1	2	0.801	0.77
0.774	2105	2	1	0.769	0.70
		3	0	0.736	
0.731	2452	1	3	0.734	0.82
0.703	2678	2	2	0.701	0.73
0.672	2928	3	1	0.669	0.55
		4	0	0.636	
0.635	3226	2	3	0.634	0.62
0.606	3460	3	2	0.602	0.80
0.569	3759	4	1	0.569	0.50
		5	0	0.537	
0.540	3992	3	3	0.535	0.55
0.505	4275	4	2	0.502	0.65
0.458	4654	5	1	0.470	0.48
		6	0	0.437	
0.437	4823	4	3	0.435	0.49
0.414	5009	5	2	0.402	0.50

[a] These tentative assignments of v_1 and v_4 are made using the best fit frequencies of 804 and 541 cm^{-1}, respectively. The calculated positions are based on these assignments and harmonic frequencies. (See Sec. IV E.)
[b] Since we assume uniform peak widths (0.022 eV), the intensity of each peak is proportional to the Franck–Condon factor (area under the peak).

heat capacity of the electron,[45,46] and the heat capacities of NO_3 and NO_3^- are estimated from the vibrational frequencies listed below (Sec. IV A).[47] We have also used those NO_3^- vibrational frequencies to calculate $\Delta_f H°(NO_3^-)_{298\ K}$ from the previously reported value of $\Delta_f H°(NO_3^-)_{391\ K} = -3.269 \pm 0.023$ eV (-75.39 ± 0.54 kcal/mol).[44] We obtain $\Delta_f H°(NO_3)_{298\ K} = -0.777 \pm 0.027$ eV (17.91 ± 0.62 kcal/mol). This does not agree with the most recent measurement of $\Delta_f H°(NO_3)_{298\ K} = 0.667 \pm 0.033$ eV (15.39 ± 0.75 kcal/mol),[48] but does agree with the previous value of 0.737 ± 0.217 eV (17.0 ± 5.00 kcal/mol).[49]

Photoelectron spectra at 266 and 213 nm were taken at two laser polarization directions, $\theta = 0°$ and 90°, where θ is the angle between the electric field vector of the laser light and the direction of electron collection. The angular distribution of the ejected photoelectrons is described by[50]

$$\frac{d\sigma}{d\omega} = \frac{\sigma_{tot}}{4\pi}\left[1 + \beta(E)\left(\frac{3}{2}\cos^2\theta - \frac{1}{2}\right)\right], \qquad (3)$$

where $\beta(E)$ is the asymmetry parameter for the electronic transition in question, E is the energy above the photodetachment threshold, and θ is the polarization angle. If relative peak intensities across a progression change significantly with θ, this may indicate the presence of overlapping electronic states or vibronic coupling effects, since β may be different for each electronic transition. The 213 nm spectra of NO_3^- are essentially the same at $\theta = 0°$ and 90°, indicating that β is approximately zero for the $^2A_2'$ and $^2E''$ transitions at this wavelength. At 266 nm, the peaks at 0.693 and 0.607 eV (363 and 1057 cm^{-1} relative to the origin at 0.738 eV) change intensity relative to the peak at 0.738 eV; at $\theta = 90°$, they are 50% and 29% more intense, respectively. The 50% change at 363 cm^{-1} is unusually large and may be due to vibronic coupling, which mixes the ground state with an excited electronic state; this is discussed in detail in Sec. IV D.

IV. ANALYSIS AND DISCUSSION

A. Background

The analysis of our NO_3^- photoelectron spectra is facilitated by the results of previous experiments on the anion and neutral. Although NO_3^- has not been studied in the gas phase, x-ray and neutron diffraction experiments on crystalline sodium nitrate indicate that the ion has D_{3h} equilibrium geometry with an average NO bond length of 1.23 Å.[28] Vibrational frequencies of NO_3^- have been measured by infrared[51,52] and Raman[52,53] spectroscopy of condensed-phase nitrates. Average values are: $\nu_1 = 1054$ cm^{-1} (symmetric stretch, a_1'), $\nu_2 = 834$ cm^{-1} (out-of-plane bend, a_2''), $\nu_3 = 1379$ cm^{-1} (antisymmetric stretch, e'), and $\nu_4 = 723$ cm^{-1} (in-plane bend, e'). The 1054 cm^{-1} mode

was not observed in the infrared spectra, nor the 834 cm^{-1} mode in Raman spectra, in accordance with the selection rules for a D_{3h} molecule. Both modes could be observed, in principle, if NO_3^- had C_{2v} or C_{3v} symmetry in the ground state.

Vibrational frequencies in the ground state of gas-phase NO_3 have been obtained from two types of experiments. In 1983, Ishiwata[7] and Nelson[8] independently reported measurements of dispersed fluorescence from excitation of the 0–0 transition in the $^2E' \leftarrow {}^2A_2'$ band, but drew conflicting conclusions from their data. Nelson assumed the NO_3 ground state to have C_{2v} symmetry. Ishiwata and coworkers interpreted the vibrational structure in the dispersed fluorescence spectrum in terms of a D_{3h} ground state, and obtained values for ν_1, ν_3, and ν_4 of 1060, 1480, and 380 cm^{-1}, respectively, for the ground state. This assignment meant that they were observing odd Δv transitions in the non-totally symmetric ν_3 and ν_4 modes, which could be explained by the Jahn–Teller coupling expected in the $^2E'$ state.

Rotationally resolved infrared absorption measurements on gas-phase NO_3[4–6] gave a more accurate value of ν_3 (1492.393 cm^{-1}) and measured the ν_2 out-of-plane bending frequency (762.327 cm^{-1})[5] for the first time. The high resolution spectra of the ν_2 and ν_3 bands exhibit rotational structure characteristic of a planar symmetric top with a threefold symmetry axis, consistent with a D_{3h} equilibrium geometry for the NO_3 ground state. No infrared absorption was observed in the vicinity of the totally symmetric ν_1 mode (1060 cm^{-1}), again consistent with D_{3h} symmetry. The pattern of rotational lines shows that the 762 cm^{-1} band is a parallel transition ($\Delta K = 0$) and the 1492 cm^{-1} band a perpendicular transition ($\Delta K = \pm 1$). The out-of-plane bend is the only infrared-active mode which should appear as a parallel band, so the 762 cm^{-1} band is confirmed to be the ν_2 mode. The rotational analysis yields an N–O bond length of 1.240 Å.

Although the rotationally resolved spectra strongly suggest a D_{3h} ground state geometry, several *ab initio* calculations[11–18] predict a Y-shaped planar C_{2v} configuration for the ground state. In addition, some of the dispersed fluorescence[8] and electron resonance[54] experimental results have been interpreted as evidence of C_{2v} symmetry. Similar discrepancies have been reported for CO_3^-,[55] which is isoelectronic with NO_3. The high resolution spectra of NO_3 rule out a rigid C_{2v} structure, because that would result in rotational structure characteristic of an asymmetric top. However, it is possible that the NO_3 ground state structure is nonrigid. This could occur, for example, if the potential energy surface had three equivalent shallow minima, each corresponding to a "Y-shaped" C_{2v} equilibrium structure. Ishiwata *et al.*[4,6] have argued against a triple-minimum potential, since that should lead to additional bands which were not observed in their spectra. We will consider this issue below.

One complication in the analysis of the high resolution spectra is the role of the excited $^2E''$ state, which had not previously been observed because the transition from the $^2A_2'$ ground state is electric-dipole forbidden. Ishiwata *et al.*[4] and Friedl and Sander[5] suggested that a very low-lying excited electronic state (less than 2000 cm^{-1} above the ground state) might account for anomalous features observed in the high resolution spectra. For example, Friedl and Sander observed an additional Q branch, which they could not assign, near the Q branch of the ν_2 band. Several *ab initio* calculations[11,16,24,25] also predict the existence of a $^2E''$ state close to the ground state. Our spectra clearly show that the $^2E''$ state lies much further above the ground state (7000 cm^{-1}).

B. NO_3 ground state: Features of the spectrum

Our understanding of the NO_3 ground state is derived from the vibrational structure observed in the 266 nm photoelectron spectrum. The peak positions and intensities in this spectrum provide information about vibrational frequencies and molecular geometry in the ground state. In the Franck–Condon approximation, the transition intensity between the vibrational levels v'' in the anion and v' in the neutral is given by[29]

$$I \propto |\tau_e|^2 |\langle \psi_{v'} | \psi_{v''} \rangle|^2. \tag{4}$$

Here τ_e is the electronic transition dipole moment between the anion electronic wave function $\Phi_{e''}$ and neutral + photoelectron wave function $\Phi_{e'}$,

$$\tau_e = \langle \Phi_{e'} | \mu_e | \Phi_{e''} \rangle \tag{5}$$

which is assumed to be constant for vibrational transitions within a single electronic band. The Franck–Condon factor $|\langle \Psi_{v'} | \Psi_{v''} \rangle|^2$, depends on the spatial overlap of ion and neutral vibrational wave functions $\psi_{v''}$ and $\psi_{v'}$. This overlap will be identically zero unless the direct product $\Gamma_{v'} \otimes \Gamma_{v''}$ contains the totally symmetric representation in the molecular point group. Transitions to all levels of totally symmetric vibrations in NO_3 are allowed from the totally symmetric ground vibrational state of NO_3^-, as are transitions to even quanta of the non-totally symmetric vibrations. The frequency of a particular non-totally symmetric mode ν_i must change substantially between the ion and neutral if transitions other than those with $v_i' = v_i''$ are to have significant intensity.[56]

Within the Franck–Condon approximation [Eq. (4)], the appearance of the NO_3^- photoelectron spectra can be predicted from relevant changes in geometry and frequency between the anion and neutral. In the ground state, the small change in N–O bond length upon photodetachment should result in a short progression in the ν_1 symmetric stretch of NO_3. No progression in the out-of-plane bend is expected, because the ion and neutral are planar with similar ν_2 frequencies. Similar reasoning applies to the ν_3 antisymmetric stretch. However, the ν_4 frequency decreases considerably upon photodetachment, from 723 to 380 cm^{-1} (assuming the assignment by Ishiwata *et al.*[7] to be correct), so that transitions with even Δv_4 might be observed.

The experimental photoelectron spectrum in Fig. 2 fulfills some of these predictions. We initially assign the intense

peak at 0.738 eV to the origin of the $^2A_2'$ band. The most intense progression appears as peaks at 0.738, 0.607, and 0.470 eV, and the average spacing of 0.134 eV (1080 cm^{-1}) corresponds to the ν_1 frequency. A second progression has peaks at 0.738, 0.693, and 0.644 eV, and the peaks at 0.607, 0.562, and 0.511 eV appear to be the associated combination band with $v_1' = 1$. The peak spacings in the second progression, of 0.045 and 0.094 eV (363 and 758 cm^{-1}), suggest a progression in the ν_4 in-plane bend. The ν_4 progression is unusual, since transitions only to even v_4 levels of NO_3 should be allowed from the $v_4'' = 0$ level of NO_3^-. The observed peak spacing should then be 720 cm^{-1}, assuming $\nu_4 = 360\,cm^{-1}$.[57] The apparent occurrence of odd Δv_4 transitions requires explanation, and the analysis described below focuses on this phenomenon.

Finally, we assign the small peak at 0.780 eV to a "hot band" originating from an excited vibrational level of the ion. Its energy is correct for the $NO_3^-(v_4'' = 1) \rightarrow NO_3(v_4' = 1)$ transition. The intensity of this hot band implies a vibrational temperature of 435 K for NO_3^-, which is somewhat higher than that expected from our experience with other ions. We do not observe intense hot bands in the ν_1 progression, because at 435 K the population of the $v_1'' = 1$ level is about six times smaller than that of the $v_4'' = 1$ level.

C. NO_3 ground state: Detailed analysis

This section describes our attempts to simulate the experimental ground-state progression within the Franck–Condon approximation, neglecting the possible effects of vibronic coupling. We consider only the ν_1 and ν_4 modes, which are assumed to be separable. The ν_1 mode is modeled as a one-dimensional harmonic oscillator in the anion and neutral, and various two-dimensional potential energy functions are used for the neutral ν_4 mode.

Eigenfunctions and eigenvalues of each potential energy function are calculated numerically. We use a variational method for the one-dimensional ν_1 calculations,[58] and a discrete variable representation (DVR)[59] procedure for the two-dimensional ν_4 calculations. The transition intensity between the anion level $v_1'' v_2'' \cdots$ and neutral level $v_1' v_2' \cdots$ is proportional to the product of Franck–Condon factors:

$$I \propto |\langle \psi_{v_1'}(Q_1) | \psi_{v_1''}(Q_1) \rangle|^2 \cdot |\langle \psi_{v_2'}(Q_2) | \psi_{v_2''}(Q_2) \rangle|^2 \cdots . \tag{6}$$

In this calculation, we neglect mixing of the neutral normal coordinates relative to those of the anion (Duschinsky rotation), and assume the same normal coordinates for both. Ervin *et al.*[60] showed that this was a reasonable approximation in analyzing the photoelectron spectrum of NO_2^-.

The simulation of the ν_1 progression is relatively simple. We assume $\nu_1 = 1057\,cm^{-1}$ in the neutral and 1054 cm^{-1} in the anion. The anion and neutral symmetric stretch potentials are assumed to be displaced by an amount $\Delta Q_1 = 6.9 \Delta r_{NO}$ (ΔQ_1 in $amu^{1/2}$ Å, Δr_{NO} in Å); this ratio was determined from the reduced mass for the ν_1 mode and the appropriate symmetry coordinate.[61] The displacement ΔQ_1 is varied, and Franck–Condon factors calculated, until the intensity distribution of the simulated ν_1 progression agrees with the experimental result. The optimal displacement, $|\Delta Q_1| = 0.21 \pm 0.05$ $amu^{1/2}$ Å, corresponds to an NO_3^- bond length of 1.21 ± 0.01 Å, assuming that $r_{NO} = 1.24$ Å in NO_3 and that the N–O bond in the ion is shorter than that in the neutral (as determined in previous experiments, Sec. IV A). This NO_3^- bond length is close to the 1.23 Å average measured for crystalline $NaNO_3$ (variation 1.21–1.24 Å).[28] The direction of displacement and the specific form of the Q_1 normal coordinate affect only the calculated N–O bond length, and not the calculated Franck–Condon factors. The same Franck–Condon factors for ν_1 are used in all our simulations.

The ν_4 progression is more difficult to reproduce in simulations. The simplest explanation for the 360 cm^{-1} peak spacing in the experimental spectrum is that the ν_4 fundamental frequency is 180 cm^{-1}, and that we observe transitions only to even overtones of the ν_4 mode, in accordance with our selection rules. With this assignment, the ν_4 transitions observed in the dispersed fluorescence spectra[7,8] would also correspond to even v_4 levels of the NO_3 ground state, so that those results could be explained without invoking vibronic coupling in the $^2E'$ state.

We simulated the NO_3^- photoelectron spectrum with $\nu_4 = 180\,cm^{-1}$ in the NO_3 ground state. The degenerate ν_4 mode is assumed to be a two-dimensional isotropic harmonic oscillator in both the anion and neutral. Since this is a nontotally symmetric mode, the normal coordinate displacement $\Delta Q_4 = 0$. Transitions other than $\Delta v_4 = 0$ would have zero intensity if not for the large frequency change between the anion and neutral (723 to 180 cm^{-1}). The resulting simulated spectrum is shown in Fig. 4. We assume Gaussian peak envelopes of FWHM 0.022 eV, determined by space charge rather than instrumental resolution. The simulation reproduces the peak positions below 0.738 eV reasonably well, but the simulated $v_4' = 4$ peak at 0.644 eV is too small. A more serious problem is that the simulation fails to reproduce the position of the hot band at 0.780 eV. Instead, hot bands appear at 0.760 eV ($v_4' = 3 \leftarrow v_4'' = 1$) and 0.805 eV

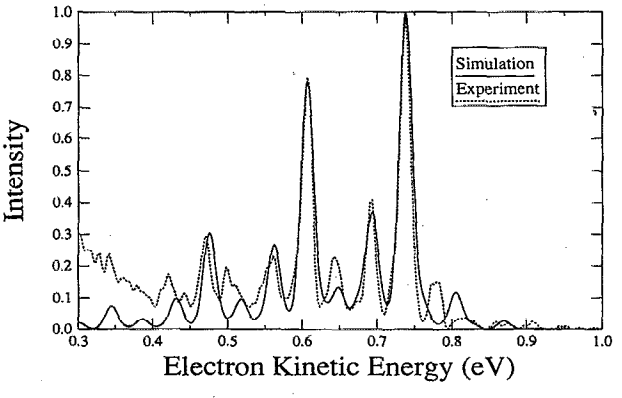

FIG. 4. Simulated photoelectron spectrum of NO_3^- (266 nm), assuming an isotropic oscillator potential for the ν_4 coordinate of NO_3. $\nu_1 = 1057\,cm^{-1}$, $\nu_1'' = 1054\,cm^{-1}$, $\nu_4 = 180\,cm^{-1}$, $\nu_4 = 723\,cm^{-1}$, $T = 435$ K.

($v_4' = 1 \leftarrow v_4'' = 1$) in the simulated spectrum. The choice of a 180 cm^{-1} isotropic oscillator for the ν_4 potential is thus unsatisfactory.

In order to gain more flexibility in simulating both the intensity distribution in this progression and the hot band position, we next consider a perturbed harmonic oscillator potential for the NO_3 ν_4 coordinate, with a barrier at the D_{3h} configuration. We use potentials of the form

$$V = \tfrac{1}{2}kr^2 - ar, \tag{7}$$

where r is the radial polar coordinate

$$r = \sqrt{Q_{4a}^2 + Q_{4b}^2} \tag{8}$$

and Q_{4a} and Q_{4b} are the degenerate components of the normal coordinate for the ν_4 mode.[62] This surface has a circular trough surrounding a barrier of height $a^2/2k$.

The energy levels of this perturbed potential differ significantly from those of the isotropic oscillator. Figure 5 shows the energy levels and associated symmetry labels for (a) a two-dimensional isotropic harmonic oscillator and (b), (c) perturbed oscillators. The energy levels in (a) show the $(n+1)$-fold degeneracy expected for the nth level of the two-dimensional isotropic oscillator. The corresponding vibrational wave functions are classified as a_1', a_2'', or e' according to their properties under the symmetry operations of the D_{3h} point group. The only transitions with nonzero Franck–Condon factors are those between levels of the same symmetry: for example, from the $a_1' v_4'' = 0$ level of the ion to a_1' levels of the neutral, or from the $e' v_4'' = 1$ level of NO_3^- to e' levels of NO_3. This restriction is equivalent to the even Δv selection rule discussed above.[63] The eigenfunctions of Eq. (7) can be classified with the same symmetry labels as the two-dimensional harmonic oscillator eigenfunctions, and the same selection rules apply. However, the perturbation due to the central barrier splits the degeneracy of levels with different symmetries, and an irregular energy level pattern results.

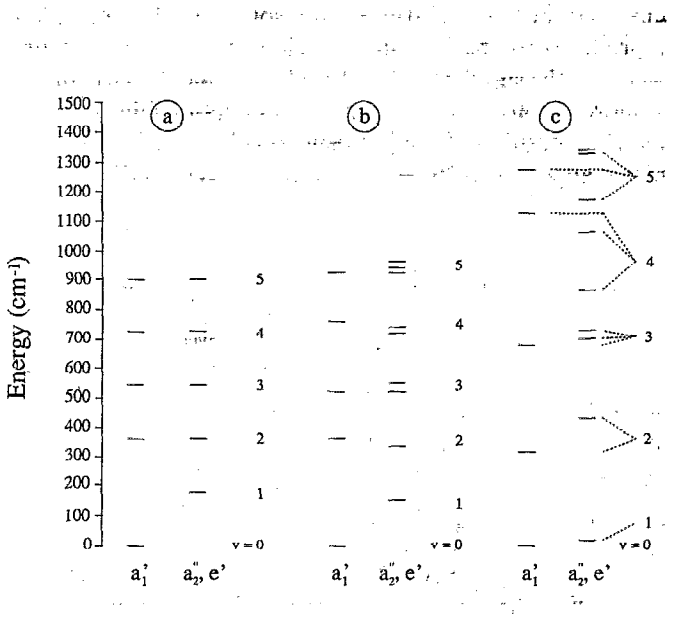

FIG. 5. Vibrational energy levels for the degenerate ν_4 mode, assuming (a) an isotropic oscillator, $\nu_4 = 180$ cm^{-1}, (b) a cylindrically symmetric potential [Eq. (7); $a = 0.065$ eV/Å, $k = 0.212$ eV/Å^2], (c) a triple-minimum potential [Eq. (9); $a = 0.340$ eV/Å, $k = 0.531$ eV/Å^2]. The isotropic oscillator energy level with $v = n$ is $(n+1)$-fold degenerate; in (b) and (c), the perturbations partially remove this degeneracy.

In our simulations assuming a potential of the form of Eq. (7), we vary both k and a (related to the unperturbed oscillator frequency and central barrier height) until the simulated peak positions and intensities agree best with the experimental spectra. In these calculations, we make the assumptions about separable modes and normal coordinates discussed above, and use the same frequencies and harmonic potential energy functions as above for ν_1 and ν_4 in NO_3 and for ν_1 in NO_3^-. Assuming the peak at 0.738 eV to be the origin, the best result is obtained for a barrier of 80 cm^{-1} ($a = 0.065$ eV/Å), with $k = 0.212$ eV/Å^2. The energy levels for this potential are shown in Fig. 5(b). The simulated spectrum is similar to that shown in Fig. 4 for the isotropic oscillator. The slightly uneven spacing of the experimental ν_4 progression is reproduced using this perturbed oscillator potential, but the simulated peak intensities and hot band positions are still not satisfactory.

Our third set of simulations assumes a triple-minimum potential energy surface for the NO_3 ν_4 coordinate, encouraged by theoretical predictions that a Y-shaped C_{2v} equilibrium geometry for NO_3 should be slightly more stable than the symmetric D_{3h} geometry.[17] We use a model potential of the form

$$V = \tfrac{1}{2}kr^2 + ar\cos 3\theta, \tag{9}$$

where r and θ are polar coordinates, r as in Eq. (8) and

$$\theta = \tan^{-1}\frac{Q_{4a}}{Q_{4b}}. \tag{10}$$

This potential energy surface has three equivalent minima at Y-shaped C_{2v} configurations, and conversion between the minima proceeds along the minimum-energy path through the D_{3h} configuration. The barrier height at the D_{3h} configuration is $a^2/2k$.

The simulations using the triple-minimum surface for ν_4 follow the procedure described above for the first perturbed oscillator. With the origin at 0.738 eV, the best result is obtained for a barrier of 210 cm^{-1}, with $k = 0.332$ eV/Å^2 and $a = 0.134$ eV/Å. The simulated spectrum is shown in Fig. 6. Although agreement with experiment is satisfactory for the peaks below 0.738 eV, the position of the hot band at 0.780 eV is incorrect.

Our problems with reproducing the intensity and position of the hot band at 0.780 eV suggest that it might instead be the origin of the $^2A_2'$ state band. This requires a higher barrier at the D_{3h} geometry, so that the 0–0 transition is no longer the most intense peak and the ν_4 progression is more extended. In this case, we assume *no* vibrational excitation in NO_3^-. The best result is obtained using a triple-minimum potential with a barrier of 870 cm^{-1} [$k = 0.531$ eV/Å^2 and $a = 0.340$ eV/Å in Eq. (9)] and is shown in Fig. 7. This simulation reproduces the positions of the major peaks in the experimental photoelectron spectrum, but the experimental intensity distribution is not reproduced as accurately as in other simulations.

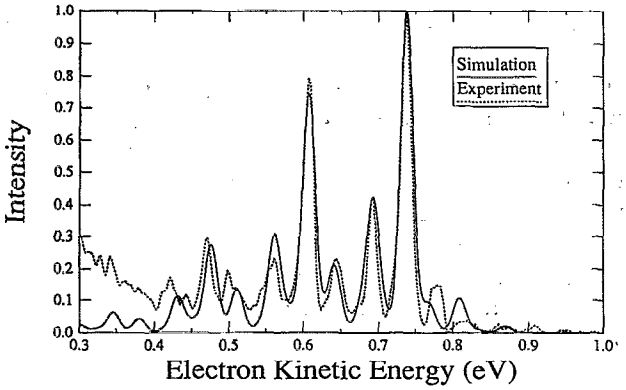

FIG. 6. Simulated photoelectron spectrum of NO_3^- (266 nm), assuming a triple-minimum potential for the ν_4 coordinate of NO_3, with a barrier of 210 cm^{-1} ($a = 0.134$ eV/Å, $k = 0.332$ eV/Å^2), origin at 0.738 eV, $T = 435$ K.

Although the simulation in Fig. 7 is the only one which reproduces the experimental peak positions including the peak at 0.780 eV, it implies a triple-minimum potential for the ν_4 coordinate, with a barrier at the D_{3h} geometry that is considerably higher than the ν_4 zero-point energy. Such a potential is inconsistent with the high resolution infrared spectra of NO_3. Figure 5(c) shows the first few energy levels of the triple-minimum potential used for the simulation of Fig. 7. The $v_4 = 1e'$ level lies only 22 cm^{-1} above the $v_4 = 0$ level, and will be substantially populated at room temperature. As discussed by Ishiwata,[4] additional hot bands originating from this level should thus occur in the infrared spectrum of the ν_3 band, due to vibration–rotation transitions between the $(v_3'' = 0, v_4'' = 1)$ and $(v_3' = 1, v_4' = 1)$ levels. These hot band transitions should be quite distinct from those transitions originating from the $(v_3'' = v_4'' = 0)$ ground state. In the ground vibrational state, only $K'' = 3n$ rotational levels have nonzero statistical weight, whereas only $K'' = 3n \pm 1$ levels have nonzero statistical weight for the $(v_3 = 0, v_4 = 1)$ vibrational level. Ishiwata *et al.*[4,6] observe only transitions with $K'' = 3n$ in the ν_3 band, ruling out a low-lying $v_4 = 1$ level such as in Fig. 5(c).

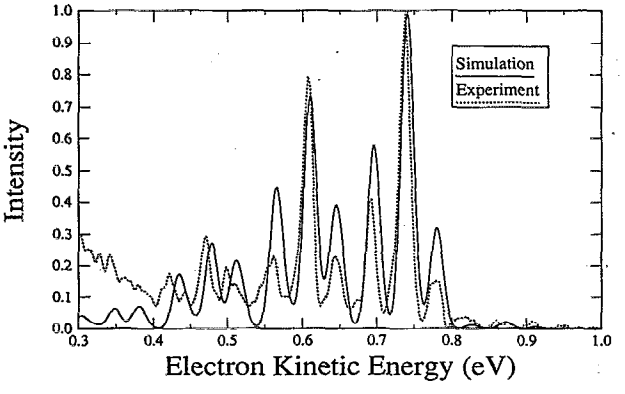

FIG. 7. Simulated photoelectron spectrum of NO_3^- (266 nm), assuming a triple-minimum potential for the ν_4 coordinate of NO_3, with a barrier of 870 cm^{-1} ($a = 0.340$ eV/Å, $k = 0.531$ eV/Å^2), origin at 0.780 eV, $T = 1$ K.

In summary, none of the simulations discussed in this section is satisfactory. We must therefore search for another explanation for the 360 cm^{-1} progression in our photoelectron spectrum.

D. Vibronic coupling in the NO_3 ground state

In this section, we consider vibronic coupling between the electronic states of NO_3 as an alternative explanation for the apparent odd Δv_4 transitions in the ground state band. Our selection rules were derived assuming nuclear and electronic motion to be separable [Eq. (4)]. Vibronic coupling makes this approximation invalid, and lends intensity to Franck–Condon forbidden transitions. The photoelectron spectrum of BF_3, which is isoelectronic with NO_3^-, shows effects similar to those that we observe. In particular, odd Δv_3 transitions are observed in the $^2A_1'$ excited state progression, due to coupling between the $^2A_1'$ and $^2E'$ states of BF_3^+. Our interpretation of our NO_3^- spectra is largely based on the comprehensive analysis of BF_3^+ by Haller *et al.*[37]

This vibronic interaction between dissimilar electronic states is called Herzberg–Teller,[64] or pseudo- (or second-order) Jahn–Teller coupling.[35,65,66] The necessary symmetry condition for a mode v to couple electronic states m and n is $\Gamma_v \otimes \Gamma_m \otimes \Gamma_n \supset \Gamma_A$,[67] where Γ_A is the totally symmetric representation in the molecular point group. In NO_3, the ν_3 and ν_4 modes ($\Gamma_v = e'$) couple the $^2A_2'$ ground state to the $^2E'$ state, and the ν_2 mode ($\Gamma_v = a_2''$) couples the $^2E'$ and $^2E''$ states. The ν_3 and ν_4 modes are also Jahn–Teller active within both the $^2E''$ and $^2E'$ states.

To examine the effects of vibronic coupling on the NO_3 ground state, we incorporate the interaction term into the molecular Hamiltonian. For simplicity, we consider only pseudo-Jahn–Teller coupling between the $^2A_2'$ and $^2E'$ electronic states (to be referred to henceforth as the A and E states) via ν_4, and neglect Jahn–Teller coupling within the $^2E'$ state. The Hamiltonian for motion in the ν_4 coordinate (using the notation of Haller *et al.*[37]) is

$$H_4^{\mathrm{PJT}} = \Omega_4 \cdot \mathbf{I}_3 + \begin{bmatrix} \varepsilon_A & \lambda_4 q_{4a} & \lambda_4 q_{4b} \\ \lambda_4 q_{4a} & \varepsilon_E & 0 \\ \lambda_4 q_{4b} & 0 & \varepsilon_E \end{bmatrix}. \quad (11)$$

Here $q_{4\alpha}$ is one of the degenerate components of the dimensionless normal coordinate q_4,[68] where

$$q_i = \sqrt{\frac{2\pi c \nu_i}{\hbar}}\, Q_i. \quad (12)$$

Ω_4 is the harmonic oscillator Hamiltonian for nuclear motion in the ν_4 mode,

$$\Omega_4 = -\frac{1}{2}\omega_4^{(A,E)}\left(\frac{\partial^2}{\partial q_{4a}^2} + \frac{\partial^2}{\partial q_{4b}^2}\right) + \frac{1}{2}\omega_4^{(A,E)}(q_{4a}^2 + q_{4b}^2), \quad (13)$$

where $\omega_4^{(A,E)}$ is the energy spacing between the unperturbed harmonic oscillator levels of the A or E state. $\mathbf{I}_3$ is the 3×3 unit matrix in the space of the A and E electronic states, λ_4 is

the pseudo-Jahn–Teller coupling constant for the ν_4 mode, and ε_i is the energy of the electronic state i. The eigenfunctions and eigenvalues of H^{PJT} can be determined using the techniques developed by Köppel *et al.*,[35] who use coupling constants and vibrational frequencies calculated by *ab initio* methods. Their "exact" methods use vibronic basis functions which are products of harmonic oscillator nuclear wave functions and diabatic electronic wave functions for the A and E states. Assuming ω_4^A and ω_4^E to be equal, the nuclear basis functions coupled by the $\lambda_4 q_{4\alpha}$ terms in H_4^{PJT} differ by one quantum of v_4.

The pseudo-Jahn–Teller interaction therefore couples the $v_4 = n$ level of the $^2A_2'$ state with the $v_4 = n \pm 1$ levels of the $^2E'$ state. This explains the odd Δv_4 transitions observed in the ground state progression. The photodetachment transition probability from the NO_3^- ground state to odd vibronic levels of NO_3 is no longer zero, since these nominally forbidden transitions borrow intensity from allowed transitions to the even v_4 levels of the $^2E'$ state. In addition, the A state vibronic levels obtain some of the character of those E state levels, which might explain the variation in the 0.693 eV (363 cm^{-1} from the origin) peak intensity with laser polarization.

We now wish to determine the coupling strength λ_4 necessary to explain the intensity distribution in our spectra. Since we do not have a reliable *ab initio* estimate of λ_4, we calculate an approximate value from the experimental peak intensities, using the expression derived by Haller *et al.*[36]

$$\frac{I_{v_1,v_4=1}(A)}{I_{v_1,v_4=0}(A)} \simeq \frac{2|\tau_{E'}|^2\lambda^2}{|\tau_A|^2} \cdot \frac{1}{(\Delta\varepsilon + \omega_4)^2}. \tag{14}$$

Here v_i is the quantum number in the ith vibrational mode, $\Delta\varepsilon \simeq \varepsilon_A - \varepsilon_{E'} = -1.87$ eV, and τ is the electronic transition dipole moment for a particular state. This is a simplified version of their expression, which is based on first-order perturbation theory approximations to the wave functions. The unperturbed frequency ω_4 is assumed to be the same in the ion and in the neutral A and E states (720 cm^{-1}). To calculate λ_4, we require the ratio $2|\tau_{E'}|^2/|\tau_A|^2$. This would be given by the ratio of the integrated intensities of the $^2E'$ and $^2A_2'$ bands in the 213 nm spectrum. Since we observe the $^2E''$ state but not the $^2E'$ state, we assume $\tau_{E'} \simeq \tau_{E''}$. The transition moment ratio is thus $2|\tau_{E'}|^2/|\tau_A|^2 \simeq 10$, the ratio of the integrated areas under the $^2E''$ and $^2A_2'$ state progressions at 213 nm. (As discussed in Sec. III, the photodetachment cross section to the $^2A_2'$ state, which is proportional to $|\tau_A|^2$, is exceptionally low.) For the $I_{v_1,v_4=1}/I_{v_1,v_4=0}$ ratio in Eq. (14) we use four peak intensity ratios measured from the NO_3 ground state progression. We use the results for $v_1 = 0$ and 1, and those at two laser polarization angles ($\theta = 0°$ and 90°).

We calculate an average value for λ_4 of 0.348 ± 0.058 eV, which is similar to the $^2A_2'$–$^2E'$ coupling constants calculated for BF_3^+. Our value of λ_4 indicates that this vibronic coupling mechanism provides a reasonable explanation for the odd Δv_4 transitions that we observe. However, the intensity borrowing effect of the pseudo-Jahn–Teller interaction in NO_3 is amplified, relative to BF_3^+, by the large $|\tau_{E'}|^2/|\tau_A|^2$ value.

If the vibronic coupling is sufficiently strong, the equilibrium geometry of the NO_3 ground state may be affected. The adiabatic electronic potentials for the A and E states should then show minima at configurations other than the symmetric D_{3h} position ($q_4 = 0$). These adiabatic potential energy surfaces, for motion along the q_4 coordinate, are determined by neglecting the nuclear kinetic energy in H^{PJT} [Eq. (11)], setting $\omega_4^A = \omega_4^E$, and diagonalizing the resulting matrix:

$$\begin{bmatrix} \varepsilon_A + \frac{1}{2}\omega_4 q_4^2 & \lambda_4 q_{4a} & \lambda_4 q_{4b} \\ \lambda_4 q_{4a} & \varepsilon_E + \frac{1}{2}\omega_4 q_4^2 & 0 \\ \lambda_4 q_{4b} & 0 & \varepsilon_E + \frac{1}{2}\omega_4 q_4^2 \end{bmatrix}, \tag{15}$$

where $q_4^2 = q_{4a}^2 + q_{4b}^2$. For a given value of λ_4, we estimate ω_4 by comparing the first few vibrational levels on the A state surface with the experimental ν_4 progression. If we set $\lambda_4 = 0.348$ (the perturbation theory value), the best agreement with experimental peak positions is obtained for $\omega_4 \simeq 0.125$ eV (1000 cm^{-1}). The experimental $v_4 = 1$ and 2 peaks are 363 and 758 cm^{-1} from the origin. The eigenvalues of the adiabatic surface reproduce this uneven spacing, but the calculated positions are 359 and 842 cm^{-1}. Decreasing λ_4 and adjusting ω_4 accordingly improves the fit. At $\lambda_4 = 0.290$ eV, the lower limit of our calculated coupling strength, $\omega_4 = 0.1$ eV (805 cm^{-1}) gives peaks at 360 and 780 cm^{-1}.

The estimate of ω_4, the unperturbed vibrational frequency, obtained from our simulations is similar to the measured $\nu_4 = 720$ cm^{-1} in NO_3^-. Vibronic coupling may thus explain the anomalously low measured ν_4 frequency in the NO_3 $^2A_2'$ state, in addition to explaining other features of the ground state progression. Figure 8 shows the adiabatic curves with and without the pseudo-Jahn–Teller interaction energy, for $\lambda_4 = 0.290$ eV and $\omega_4^A (= \omega_4^E) = 0.1$ eV (805

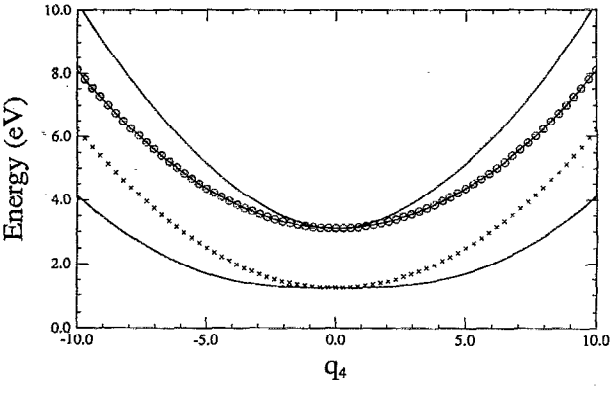

FIG. 8. Potential energy of the NO_3 $^2A_2'$ and $^2E'$ states as a function of q_4, the dimensionless normal coordinate. The solid curves are the adiabatic pseudo-Jahn–Teller-perturbed potentials calculated from Eq. (15), with $\omega_4 = 0.1$ eV (805 cm^{-1}) and $\lambda_4 = 0.290$ eV. We have neglected Jahn–Teller coupling in the $^2E'$ state. The unperturbed harmonic oscillator potentials for the $^2A_2'$ (×) and $^2E'$ (○) states are also shown.

cm^{-1}). One of the components of the $^2E'$ state is not affected by the perturbation, but the other interacts repulsively with the $^2A_2'$ state.

This perturbed potential for the A state has a minimum at $q_4 = 0$, corresponding to a D_{3h} equilibrium geometry. Haller *et al.*[37] have shown that this will be true as long as $\lambda_4^2/\omega_4 \leq \frac{1}{2}(\varepsilon_E - \varepsilon_A)$. Even with $\lambda_4 = 0.348$ eV and $\omega_4 = 0.125$ eV, the barrier in the adiabatic potential is only 0.001 eV. We believe that our lower estimate of λ (0.290 eV), which gives a better fit to the experimental peak spacings, is closer to the true PJT coupling constant. To obtain the transition moment ratio $|\tau_{E'}|^2/|\tau_A|^2$ used in Eq. (14), we assumed that $|\tau_{E'}|^2 = |\tau_{E''}|^2$. It is likely that the $^2E''$ and $^2E'$ states have somewhat different integrated intensities, so the perturbation theory estimate of $\lambda_4 = 0.348$ eV is a good first guess, at best. The coupling constant derived from fitting peak spacings is more reliable because we are then using experimental information to adjust λ_4 and ω_4. The comparison of adiabatic eigenvalues to experimental peak spacings is not strictly valid, since nonadiabatic coupling due to the nuclear kinetic energy operator will mix vibronic levels of the individual A and E surfaces.[66,69] However, the $v_4 = 0$, 1, and 2 levels of the A state lie well below the E state, so nonadiabatic effects on these low-lying states are probably small. Our calculated vibronic coupling strength is sufficient to induce intensity in forbidden transitions, but is weak enough that the NO_3 $^2A_2'$ state still has D_{3h} symmetry.

In summary, pseudo-Jahn–Teller coupling between the $^2A_2'$ and $^2E'$ states of NO_3 via the ν_4 mode accounts for the observed peak positions in the ground state band of the NO_3^- photoelectron spectrum. The coupling strength necessary to reproduce our results does not break the D_{3h} symmetry of the $^2A_2'$ state, and this explanation is consistent with the D_{3h} equilibrium geometry implied by the high resolution spectra of NO_3. An important test of our analysis should result from obtaining a photoelectron spectrum which includes the $^2E'$ state of NO_3. This will allow the direct measurement of $2|\tau_{E'}|^2/|\tau_A|^2$, the parameter which controls intensity borrowing via pseudo-Jahn–Teller coupling. This experiment should be possible using an ArF excimer laser (photon energy 6.42 eV).

E. NO_3 excited state

The 213 nm spectrum of NO_3^- shows an excited state progression 0.868 ± 0.014 eV (7000 ± 110 cm^{-1}) above the ground state. This is identified as the $^2E''$ state of NO_3, since the $^2E'$ state has been observed at 1.87 eV[7,8,21,23,70] and the dark $^2E''$ state is predicted to lie between the ground state and $^2E'$ state. The $^2E''$ band shows extensive vibrational structure. A satisfactory fit to the peak positions is obtained by assuming only two active harmonic vibrational modes, with frequencies of 804 ± 4 cm and 541 ± 8 cm^{-1}; the 804 cm^{-1} progression is considerably longer.

We first try to assign these two progressions by comparing their frequencies to those observed in NO_3^- and other electronic states of NO_3. Since the $^2E''$ state is degenerate, the degenerate ν_3 and ν_4 modes can be activated in the photoelectron spectrum via first-order Jahn–Teller coupling, which allows odd Δv transitions to occur in these modes. As discussed above, a change in the N–O bond length upon photodetachment to the $^2E''$ state will also lead to a progression in the ν_1 symmetric stretch. If vibronic interactions between the $^2E''$ state and other electronic states are negligible, the ν_2 out-of-plane bending mode should not be active since the $^2E''$ state is expected to be planar.

The measured ν_4 frequencies in NO_3^- and in the $^2A_2'$ state of NO_3 are 723 and 360 cm^{-1}, respectively, so either the 541 or the 804 cm^{-1} frequency in the $^2E''$ band could correspond to the ν_4 mode. The ν_1 frequency is about 1060 cm^{-1} in the ion and neutral ground state, and 950 cm^{-1} in the neutral $^2E'$ state,[20,70] but the average ν_3 frequency in the ion and two neutral states is 1440 cm^{-1}. Assuming that these are the only possible active modes, the most reasonable assignment on the basis of frequency alone is that the 804 cm^{-1} progression corresponds to the ν_1 mode and the 541 cm^{-1} progression to the ν_4 mode. Using this assignment, Table II lists the v_1 and v_4 quantum numbers for each peak in the band. With this assignment, the $v_4' = 1 \leftarrow v_4'' = 1$ transition, which is prominent in the $^2A_2'$ state progression, should occur at 1.060 eV. The 0–0 peak at 1.038 eV does have a shoulder in the right place for this hot band transition.

We next consider the intensity distribution in the $^2E''$ band. Table II lists peak intensities relative to the $(v_1 = 1, v_4 = 0)$ peak at 0.935 eV (calculated position). These were obtained by assuming Gaussian peaks, each of FWHM 0.022 eV, and determining the peak intensities required for the cumulative simulated spectrum to match the experimental spectrum. Peak positions were calculated from the harmonic frequencies. Figure 9 shows that we can reproduce the peak positions and the broad, intense base under the $^2E''$ band with overlapped Gaussians.

The intensity distribution in Table II presents two problems. If we assume that the two modes are separable, the intensity of each peak should be given by a product of Franck–Condon factors as in Eq. (6). The intensity ratio for the peaks $(v_1 = n, v_4)$ and $(v_1 = m, v_4)$ is then independent

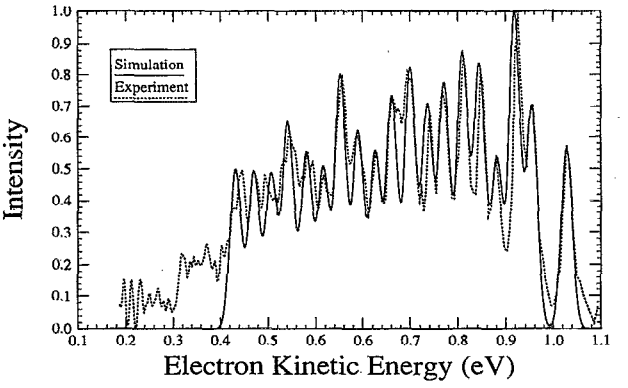

FIG. 9. Experimental and "simulated" photoelectron spectra of NO_3^- (213 nm), for detachment to the NO_3 $^2E''$ state. The simulation assumes two active modes, of frequency 804 and 541 cm^{-1}, and shows that a combination of Gaussian peaks (FWHM 0.022 eV) can reproduce the peak positions and shape of the $^2E''$ band.

of v_4. However, the observed (1,0)/(0,0) ratio is 1.75, the (1,1)/(0,1) ratio is 1.19, and the (1,2)/(0,2) ratio is 1.45. Similar discrepancies occur throughout the band.

In addition, if we assume the ν_1 mode to be a one-dimensional harmonic oscillator displaced from the oscillator in the ion, which is appropriate for a totally symmetric mode, we are unable to model the $(n,0)$ progression. Specifically, if we match the experimental (1,0)/(0,0) ratio the simulated peak intensities for $v_1 \geqslant 4$ are considerably lower than the experimental intensities. If we assume that $\Delta Q_1 = 6.9\ \Delta r_{NO}$ for the $^2E''$ state, as we did for the $^2A_2'$ state (Sec. IV C), the displacement necessary to match the experimental (1,0)/(0,0) ratio requires that the N–O bond length change by 0.07 Å between the ion and the $^2E''$ state. This seems excessive for the removal of a nominally nonbonding e'' electron[3] from the ion. (By comparison, removal of a nonbonding a_2' electron in the transition from NO_3^- to the $^2A_2'$ state results in a bond length change of only about 0.03 Å.)

The intensity distribution in the $^2E''$ band shows that separability of the two active modes in the $^2E''$ state is a poor assumption. This leads us to question our assignment of the 804 cm^{-1} progression to the symmetric stretch, since the ν_1 and ν_4 modes are of different symmetries and should not mix. An alternative explanation for this progression involves vibronic coupling with other electronic states. In Sec. IV D, the ν_4 progression in the $^2A_2'$ band was attributed to pseudo-Jahn–Teller coupling between the $^2A_2'$ and $^2E'$ states via the ν_4 mode. This vibronic coupling mechanism also exists between the $^2E''$ and $^2E'$ states via the ν_2 out-of-plane bend (a_2'' symmetry) and can activate the ν_2 mode in the $^2E''$ band. The ν_2 frequency is 834 cm^{-1} in NO_3^- and 762 cm^{-1} in the NO_3 $^2A_2'$ state, so the 804 cm^{-1} progression in the $^2E''$ state is in the right frequency range for the ν_2 mode. If this assignment were correct, the extended nature of the 804 cm^{-1} progression would imply substantial vibronic coupling, possibly large enough to cause distortion from a planar equilibrium geometry for the $^2E''$ state. However, Haller *et al.*[37] calculated the analogous pseudo-Jahn–Teller coupling constant for BF_3^+ to be relatively small. In addition, the absence of the $^2E'' \leftarrow {}^2A_2''$ transition in absorption puts a limit on the strength of the coupling between the $^2E'$ and $^2E''$ states.

More theoretical work on NO_3 is required before we can determine whether this alternative assignment is realistic. Ideally, vibronic coupling constants could be obtained by *ab initio* methods, and then used in calculations of the type developed by Cederbaum and co-workers.[35] These simulations of the $^2E''$ band should clearly indicate the relative importance of different vibronic coupling mechanisms.

V. SUMMARY AND CONCLUSIONS

We have observed the $^2A_2'$ ground state and $^2E''$ first excited state of NO_3 via photoelectron spectroscopy of the NO_3^- anion. The electron affinity of NO_3 is 3.937 ± 0.014 eV, and we calculate $\Delta_f H°(NO_3)_{298\ K} = 0.777 \pm 0.023$ eV (17.91 ± 0.62 kcal/mol). Our analysis of the $^2A_2'$ band indicates that the NO_3 ground state has a D_{3h} equilibrium geometry, but is perturbed by vibronic coupling to the $^2E'$ second excited electronic state through the ν_4 degenerate in-plane bend. This coupling explains both the appearance of odd Δv_4 transitions in this band and the anomalously low ν_4 vibrational frequency in the $^2A_2'$ state.

Our results represent the first direct observation of the $^2E''$ state of NO_3, which lies 0.868 ± 0.027 eV above the ground state. The $^2E''$ band shows extensive vibrational structure which has been tentatively assigned to progressions in the ν_1 symmetric stretch and the Jahn–Teller active ν_4 mode. However, this assignment is not completely satisfactory, and the analysis of the $^2E''$ band could clearly benefit from further theoretical work.

ACKNOWLEDGMENTS

This research is supported by the Air Force Office of Scientific Research under Grant No. AFOSR-87-0341. We thank R. Boehm, H. F. Davis, R. Davy, E. Hirota, K. Kawaguchi, B. Kim, W. C. Lineberger, and H. F. Schaefer for communicating their results prior to publication, and also H. Köppel for helpful discussions.

[1] *Atmospheric Ozone 1985: Assessment of Our Understanding of the Processes Controlling its Present Distribution and Change*, World Meteorological Organization, Global Ozone Research and Monitoring Project-Report No. 16 (NASA, Washington, D.C., 1985), pp. 32–35.
[2] J. H. Seinfeld, Science **243**, 745 (1989); S. E. Schwartz, *ibid.* **243**, 753 (1989); M. B. McElroy and R. J. Salawitch, *ibid.* **243**, 763 (1989).
[3] A. D. Walsh, J. Chem. Soc. **1953**, 2301.
[4] T. Ishiwata, I. Tanaka, K. Kawaguchi, and E. Hirota, J. Chem. Phys. **82**, 2196 (1985).
[5] R. R. Friedl and S. P. Sander, J. Phys. Chem. **91**, 2721 (1987).
[6] K. Kawaguchi, E. Hirota, T. Ishiwata, and I. Tanaka, J. Chem. Phys. **93**, 951 (1990).
[7] T. Ishiwata, I. Fujiwara, Y. Naruge, K. Obi, and I. Tanaka, J. Phys. Chem. **87**, 1349 (1983).
[8] H. H. Nelson, L. Pasternack, and J. R. McDonald, J. Phys. Chem. **87**, 1286 (1983).
[9] A. Lund and K.-Å. Thuomas, Chem. Phys. Lett. **44**, 569 (1976).
[10] N. C. Baird and K. F. Taylor, Chem. Phys. Lett. **80**, 83 (1981).
[11] R. C. Boehm and L. L. Lohr, J. Phys. Chem. **93**, 3430 (1989).
[12] R. C. Boehm and L. L. Lohr, J. Comput. Chem. (submitted).
[13] U. Kaldor, Chem. Phys. Lett. **166**, 599 (1990).
[14] J. F. Olsen and L. Burnelle, J. Am. Chem. Soc. **92**, 3659 (1970).
[15] M. J. S. Dewar and H. S. Rzepa, J. Am. Chem. Soc. **100**, 784 (1978).
[16] P. E. M. Siegbahn, J. Comput. Chem. **6**, 182 (1985).
[17] R. D. Davy and H. F. Schaefer III, J. Chem. Phys. **91**, 4410 (1989).
[18] B. Kim, B. L. Hammond, W. A. Lester, Jr., and H. S. Johnston, Chem. Phys. Lett. **168**, 131 (1990).
[19] E. J. Jones and O. R. Wulf, J. Chem. Phys. **5**, 873 (1937).
[20] D. A. Ramsay, Proc. Colloq. Spectrosc. Int. **10**, 583 (1962).
[21] R. A. Graham and H. S. Johnston, J. Phys. Chem. **82**, 254 (1978).
[22] H. H. Nelson, L. Pasternack, and J. R. McDonald, J. Chem. Phys. **79**, 4279 (1983).
[23] W. J. Marinelli, D. M. Swanson, and H. S. Johnston, J. Chem. Phys. **76**, 2864 (1982).
[24] T. E. H. Walker and J. A. Horsley, Mol. Phys. **21**, 939 (1971).
[25] B. Kim, H. S. Johnston, D. A. Clabo, Jr., and H. F. Schaefer III, J. Chem. Phys. **88**, 3204 (1988).
[26] R. Lefebvre and E. Ressayre, Theor. Chim. Acta **18**, 31 (1970).
[27] M. Hotokka and P. Pyykkö, Chem. Phys. Lett. **157**, 415 (1989), and references within; H. Teramae, K. Tanaka, K. Shiotani, and T. Yamabe, Solid State Commun. **46**, 633 (1983); L. Radom, Aust. J. Chem. **29**, 1635 (1976).
[28] G. L. Paul and A. W. Pryor, Acta Crystallogr. B **27**, 2700 (1971); P. Cherin, W. C. Hamilton, B. Post, Acta Crystallogr. **23**, 455 (1967), and references within.
[29] J. W. Rabalais, *Principles of Ultraviolet Photoelectron Spectroscopy* (Wiley, New York, 1977), p. 53.

[30] H. C. Longuet-Higgins, Adv. Spectrosc. **2**, 429 (1961).
[31] H. C. Longuet-Higgins, U. Öpik, M. H. L. Pryce, and R. A. Sack, Proc. R. Soc. London Ser. A **244**, 1 (1958).
[32] S. D. Brossard, P. G. Carrick, E. L. Chappell, S. C. Hulegaard, and P. C. Engelking, J. Chem. Phys. **84**, 2459 (1986).
[33] W. C. Lineberger (unpublished results).
[34] P. C. Engelking and W. C. Lineberger, J. Chem. Phys. **67**, 1412 (1977).
[35] H. Köppel, W. Domcke, and L. S. Cederbaum, Adv. Chem. Phys. **57**, 59 (1984).
[36] E. Haller, H. Köppel, L. S. Cederbaum, G. Bieri, and W. von Niessen, Chem. Phys. Lett. **85**, 12 (1982).
[37] E. Haller, H. Köppel, L. S. Cederbaum, W. von Niessen, and G. Bieri, J. Chem. Phys. **78**, 1359 (1983).
[38] Reference 29, pp. 243–251.
[39] R. B. Metz, A. Weaver, S. E. Bradforth, T. N. Kitsopoulos, and D. M. Neumark, J. Phys. Chem. **94**, 1377 (1990).
[40] M. A. Johnson and W. C. Lineberger, in *Techniques of Chemistry, Vol. 20: Techniques for Study of Ion–Molecule Reactions*, edited by J. M. Farrar and W. H. Saunders, Jr. (Wiley, New York, 1988), p. 591.
[41] T. N. Kitsopoulos, I. M. Waller, J. G. Loeser, and D. M. Neumark, Chem. Phys. Lett. **159**, 300 (1989).
[42] W. C. Wiley and I. H. McLaren, Rev. Sci. Instrum. **26**, 1150 (1955).
[43] H. Hotop and W. C. Lineberger, J. Phys. Chem. Ref. Data **14**, 731 (1985).
[44] J. A. Davidson, F. C. Fehsenfeld, and C. J. Howard, Int. J. Chem. Kinet. **9**, 17 (1977).
[45] S. G. Lias, J. E. Bartmess, J. F. Liebman, J. L. Holmes, R. D. Levin, and W. G. Mallard, J. Phys. Chem. Ref. Data **17**, Suppl. 1 5–30 (1988).
[46] M. W. Chase, Jr., C. A. Davies, J. R. Downey, Jr., D. J. Frurip, R. A. McDonald, and A. N. Syverud, J. Phys. Chem. Ref. Data **14**, Suppl. I 10–18 (1985).
[47] E. B. Wilson, Jr., Chem. Rev. **27**, 17 (1940).
[48] A. H. McDaniel, J. A. Davidson, C. A. Cantrell, R. E. Shetter, and J. G. Calvert, J. Phys. Chem. **92**, 4172 (1988).
[49] Reference 46, p. 1537, and references within.
[50] J. Cooper and R. N. Zare, J. Chem. Phys. **48**, 942 (1968).
[51] N. Smyrl and J. P. Devlin, J. Phys. Chem. **77**, 3067 (1973); R. Kato and J. Rolfe, J. Chem. Phys. **47**, 1901 (1967); V. Narayanamurti, W. D. Seward, and R. O. Paul, Phys. Rev. **148**, 481 (1966); A. K. Ramdas, Proc. Ind. Acad. Sci. A **37**, 441 (1953).
[52] J. D. Riddell, D. J. Lockwood, and D. E. Irish, Can. J. Chem. **50**, 2951 (1972); G. Pollard, N. Smyrl, and J. P. Devlin, J. Phys. Chem. **76**, 1826 (1972).
[53] B. S. Rama Rao, Proc. Ind. Acad. Sci. A **10**, 167 (1939); P. A. Moses, *ibid.* A **10**, 71 (1939); M. J. Chédin, J. Phys. Radium, Vol. V. Ser. VII, 445 (1939); R. Ananthakrishnan, Proc. Ind. Acad. Sci. A **5**, 447 (1937).
[54] (a) C_{2v} symmetry: G. W. Chantry, A. Horsfield, J. R. Morton, and D. H. Whiffen, Mol. Phys. **5**, 589 (1962). (b) D_{3h} symmetry: D. E. Wood and G. P. Lozos, J. Chem. Phys. **64**, 546 (1976); T. W. Martin, L. L. Swift, and J. H. Venable, Jr., *ibid.* **52**, 2138 (1970); R. Livingston and H. Zeldes, *ibid.* **41**, 4011 (1964); (c) A. Reuveni and Z. Luz, J. Magn. Reson. **23**, 271 (1976): unable to determine.
[55] J. T. Snodgrass, C. M. Roehl, P. A. M. van Koppen, W. E. Palke, and M. T. Bowers, J. Chem. Phys. **92**, 5935 (1990), and references within.
[56] G. Herzberg, *Molecular Spectra and Molecular Structure III: Electronic Spectra and Electronic Structure of Polyatomic Molecules* (Van Nostrand Reinhold, New York, 1966), p. 152.
[57] This 360 cm^{-1} frequency is based on our spectra and dispersed fluorescence results of Nelson *et al.* (Ref. 8) and Kim *et al.* [B. Kim, P. Hunter, H. S. Johnston (manuscript in preparation)]. Ishiwata *et al.* (Ref. 7) measured 380 cm^{-1} in their dispersed fluorescence spectra, but this small difference in frequency does not affect the essential details of our analysis.
[58] R. B. Metz (Chemistry Dept., University of California, Berkeley), from the Franck–Condon factor program of Dr. G. B. Ellison; T. E. Sharp and H. M. Rosenstock, J. Chem. Phys. **41**, 3453 (1964); E. Hutchisson, Phys. Rev. **36**, 410 (1930).
[59] R. B. Metz (Chemistry Dept., University of California, Berkeley); J. C. Light, I. P. Hamilton, and J. V. Lill, J. Chem. Phys. **82**, 1400 (1985).
[60] K. M. Ervin, J. Ho, and W. C. Lineberger, J. Phys. Chem. **92**, 5405 (1988).
[61] E. B. Wilson, Jr., J. C. Decius, and P. C. Cross, *Molecular Vibrations* (Dover, New York, 1980), p. 309.
[62] G. Herzberg, *Molecular Spectra and Molecular Structure II: Infrared and Raman Spectra of Polyatomic Molecules* (Van Nostrand Reinhold, New York, 1945), p. 179.
[63] Although the NO_3^- $v_4'' = 0$ level and the neutral $v_4' = 3$ level, for example, both have components of a_1' symmetry, this $\Delta v = 3$ transition is not allowed. The neutral level has vibrational angular momentum $l = 1$ and has zero overlap with the $v_4'' = 0, l = 0$ level of the ion.
[64] J. M. Hollas, *High Resolution Spectroscopy* (Butterworths, London, 1982), p. 388.
[65] M. Z. Zgierski and M. Pawlikowski, J. Chem. Phys. **70**, 3444 (1979); J. H. van der Waals, A. M. D. Berghuis, and M. S. de Groot, Mol. Phys. **21**, 497 (1971); J. H. van der Waals, A. M. D. Berghuis, and M. S. de Groot, Mol. Phys. **13**, 301 (1967).
[66] H. Köppel, L. S. Cederbaum, and W. Domcke, J. Chem. Phys. **89**, 2023 (1988).
[67] Reference 56, p. 67.
[68] S. Califano, *Vibrational States* (Wiley, New York, 1976), p. 35.
[69] H. Köppel, L. S. Cederbaum, W. Domcke, and W. von Niessen, Chem. Phys. **37**, 303 (1979).
[70] D. N. Mitchell, R. P. Wayne, P. J. Allen, R. P. Harrison, and R. J. Twin, J. Chem. Soc. Faraday Trans. 2 **76**, 785 (1980).